

## Cr(Al)N/Al<sub>2</sub>O<sub>3</sub> nanocomposite coatings fabricated by differential pumping cosputtering

Masahiro Kawasaki<sup>1</sup>, Masateru Nose<sup>2</sup>, Ichiro Onishi<sup>3</sup>, Kenji Matsuda<sup>4</sup>, and Makoto Shiojiri<sup>4,5\*</sup>

<sup>1</sup> JEOL USA Inc., 11 Dearborn Road, Peabody, MA 01960, USA.

<sup>2</sup> Faculty of Art and Design, University of Toyama, Takaoka, Toyama 933-8588, Japan.

<sup>3</sup> JEOL Ltd. 3-1-2 Musashino, Akishima, Tokyo 196-8558, Japan

<sup>4</sup> School of Science and Engineering, University of Toyama, Toyama 930-8555, Japan

<sup>5</sup> Kyoto Institute of Technology, Kyoto 606-8585, Japan.

\* Present address: 1-297 Wakiyama, Kyoto 618-0091, Japan.

Nanocomposite films of metal nitrides such as TiN/Si<sub>3</sub>N<sub>4</sub>, TiN/BN, and CrN/AlN have attracted substantial attention as new hard coating materials. It is difficult to prepare composite films consisting of nitride and oxide by conventional reactive sputtering methods. Nose *et al.* developed a differential pumping cosputtering (DPCS) system with two chambers A and B, which can fabricate different nanocomposite films [1]. We elucidated the process and mechanism of film growth in the DPCS system, using Cr(Al)N/SiO<sub>x</sub> nanocomposite layer deposited on the under buffer layers grown on a Si substrate [2-4]. Here, we report the mechanical property and structure of Cr(Al)N/Al<sub>2</sub>O<sub>3</sub> layers prepared at various conditions in the DPCS system, to demonstrate its usefulness for fabricating superhard coatings.

Cr<sub>50</sub>Al<sub>50</sub> and Al<sub>2</sub>O<sub>3</sub> targets were set in chambers A and B respectively, and a (001) Si wafer was used as the substrate. The substrate was heated at 250°C. First, three depositions were successively performed on the Si substrate for making the transition or buffer layers to promote adhesion between the composite layer and substrate. Except for a substrate rotational speed of  $\omega=12$  rpm, the preparation conditions of the gas flow and RF power for these transition layers were the same as that used for the previous Cr(Al)N/SiO<sub>x</sub> nanocomposite coating [2-4]. Next, the main deposition was carried out for 810 min by operating both the CrAl chamber A and the Al<sub>2</sub>O<sub>3</sub> chamber B, on the transition layers rotated at the same speed  $\omega$ . The CrAl sputtering and the Al<sub>2</sub>O<sub>3</sub> sputtering were performed with flows of Ar (10 sccm)+N<sub>2</sub> (20 sccm) and Ar (20 sccm) respectively, at different RF powers for preparing composite layers with different compositions: *e.g.* 200 W and 100 W, respectively so as to obtain a nominal composition of Cr(Al)N/17 vol.%Al<sub>2</sub>O<sub>3</sub>. The structure was observed by analytical electron microscopy using JEOL JEM-2800 and ARM200F microscopes, and the indentation hardness  $H_{IT}$  and Young's modulus  $E^*$  of the films were measured using a nanoindentation system (Fischerscope, H100C-XYp) at room temperature.

We got the following conclusion from the experiments such as shown in Figures 1-4. (1) The transition or buffer layers prepared successively on the Si substrate by sputtering from the CrAl target with flows of (i) Ar (10 sccm), (ii) Ar (10 sccm)+N<sub>2</sub> (10 sccm), and (iii) Ar (10 sccm)+N<sub>2</sub> (20 sccm) were layers of composed of *bcc* Cr crystallites and *a*-Al<sub>2</sub>O<sub>3</sub> particles (layer C), Cr crystallites, NaCl-type CrN crystallites, and *a*-Al<sub>2</sub>O<sub>3</sub> particles (D), and Cr(Al)N crystallites and *a*-Al<sub>2</sub>O<sub>3</sub> particles (E), respectively. These layers, where the composition gradually changes from metal (Cr) to nitride (CrN), are appropriate to the adhesion between the metal substrate and the composite nitride layer. The multilayered structure composed of Cr (or CrN) layers and oxide layers, which were found in the layers prepared at  $\omega=1$  rpm, was not observed in the present layers prepared at first rotational speeds. (2) The main layer (F) grew in a columnar structure normal to the substrate surface. Each column comprises Cr(Al)N crystallites and *a*-Al<sub>2</sub>O<sub>3</sub> particles. The Cr(Al)N crystallites and *a*-Al<sub>2</sub>O<sub>3</sub> particles were homogeneously dispersed and

any multilayered structure was not formed, unlike the nanocomposite layers prepared at  $\omega = 1$  rpm. (3)  $H_{IT}$  and  $E^*$  increased with increasing  $\omega$  within a measured range of 1~12 rpm. In the multilayered structure prepared at low rotational speeds, the nitride crystal lattices in the same layer can easily deform without interrupt by oxides and the oxide particle layers also act on softening the coating. With increasing oxide fraction,  $H_{IT}$  and  $E^*$  increased to reach maximum values and then decreased. This shows that the hardness of nitride coatings is improved by fabricating the nanocomposite layer. The Cr(Al)N/17 vol. %Al<sub>2</sub>O<sub>3</sub> and Cr(Al)N/17 vol %SiO<sub>x</sub> layers prepared at  $\omega=12$  rpm were superhard coatings with  $H_{IT} = 44\sim 46$  GPa and  $E^* \sim 350$  GPa. They had the structure described in (2). The fine  $\alpha$ -Al<sub>2</sub>O<sub>3</sub> particles can work as obstacles against the lattice deformation of Cr(Al)N. The increasing amount of amorphous oxide (>17 vol. %) reduced the supremacy of hard nitride and consequently softens the coatings. Thus, we demonstrated that the DPS system allows us to fabricate superhard nanocomposite coatings with a hardness of as high as 45 GPa. Since we have prepared a composite layer with a hardness of 48 GPa, DPCS has potential to fabricate harder coating layers by controlling preparation condition and searching target materials.

- [1] M. Nose *et al*, J. Vac. Sci. Technol. A **30** (2012) 011502.  
 [2] M. Kawasaki *et al*, ACS Appl. Mater. Interfaces **5** (2013) 3833.  
 [3] M. Kawasaki *et al*, Appl. Phys. Lett. **103** (2013) 201913.  
 [4] M. Kawasaki *et al*, M&M 2014 Abstract, Hartford CT. 0383-000160.

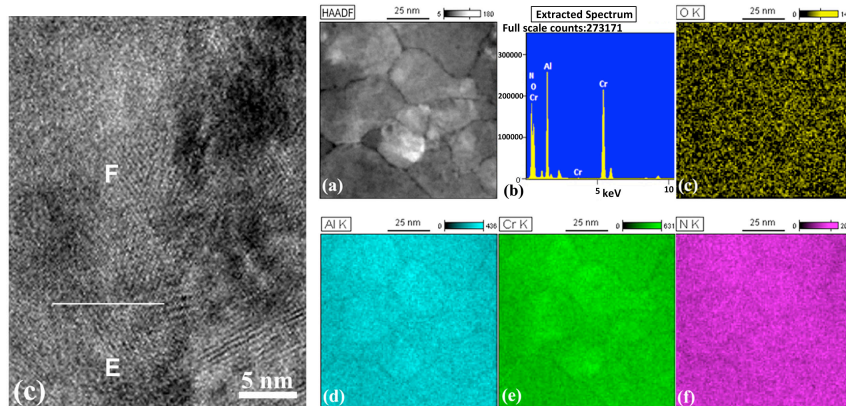
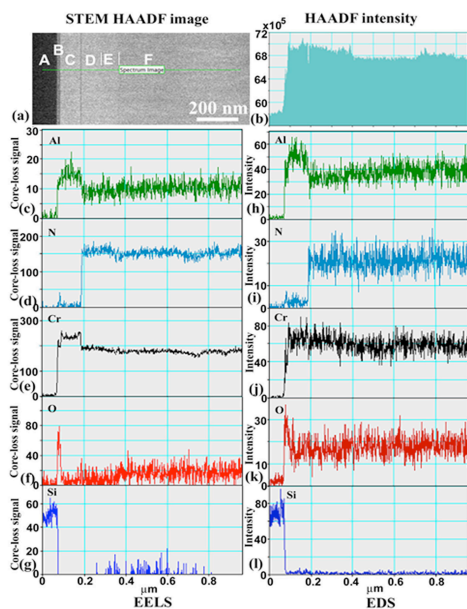


**Figure 1(top left).** (a) STEM-HAADF image of an area including layers A–F. (b) HAADF intensity profile, (c–g) EELS intensity profiles, and (h–l) EDS intensity profiles along the line indicated in (a).

**Figure 2(top middle).** HR-TEM image of an area including layers E and F.

**Figure 3(top right).** (a) STEM-HAADF image of a cross section, parallel to the substrate surface, of layer F. (b) EDS spectrum from area in (a). (c–f) EDS maps of O–K, Al–K, Cr–K, and N–K signals of the same cross section, respectively.

**Figure 4 (bottom left).**  $H_{IT}$  and  $E^*$  of Cr(Al)N/17vol.%Al<sub>2</sub>O<sub>3</sub> composite layers and Cr(Al)N layers prepared at different substrate rotational speeds.  $H_{IT}$  and  $E^*$  of Cr(Al)N/17 vol.%SiO<sub>x</sub>, and Cr(Al)N/38 vol.%SiO<sub>x</sub> layers are added for reference.

